



HAL
open science

Cosmic radio-noise absorption bursts caused by solar wind shocks

A. Osepian, S. Kirkwood

► **To cite this version:**

A. Osepian, S. Kirkwood. Cosmic radio-noise absorption bursts caused by solar wind shocks. *Annales Geophysicae*, 2004, 22 (8), pp.2973-2987. hal-00317596

HAL Id: hal-00317596

<https://hal.science/hal-00317596>

Submitted on 18 Jun 2008

HAL is a multi-disciplinary open access archive for the deposit and dissemination of scientific research documents, whether they are published or not. The documents may come from teaching and research institutions in France or abroad, or from public or private research centers.

L'archive ouverte pluridisciplinaire **HAL**, est destinée au dépôt et à la diffusion de documents scientifiques de niveau recherche, publiés ou non, émanant des établissements d'enseignement et de recherche français ou étrangers, des laboratoires publics ou privés.

Cosmic radio-noise absorption bursts caused by solar wind shocks

A. Osepian¹ and S. Kirkwood²

¹Polar Geophysical Institute, Halturina 15, Murmansk, Russia

²Swedish Institute of Space Physics, Box 812, 98128 Kiruna, Sweden

Received: 14 October 2003 – Revised: 7 April 2004 – Accepted: 20 April 2004 – Published: 7 September 2004

Abstract. Bursts of cosmic noise absorption observed at times of sudden commencements (SC) of geomagnetic storms are examined. About 300 SC events in absorption for the period 1967–1990 have been considered. It is found that the response of cosmic radio-noise absorption to the passage of an interplanetary shock depends on the level of the planetary magnetic activity preceding the SC event and on the magnitude of the magnetic field perturbation associated with the SC (as measured in the equatorial magnetosphere). It is shown that for SC events observed against a quiet background ($K_p < 2$), the effects of the SC on absorption can be seen only if the magnitude of the geomagnetic field perturbation caused by the solar wind shock exceeds a threshold value ΔB_{th} . It is further demonstrated that the existence of this threshold value, ΔB_{th} , deduced from experimental data, can be related to the existence of a threshold for exciting and maintaining the whistler cyclotron instability, as predicted by quasi-linear theory. SC events observed against an active background ($K_p > 2$) are accompanied by absorption bursts for all magnetic field perturbations, however small. A quantitative description of absorption bursts associated with SC events is provided by the whistler cyclotron instability theory.

Key words. Ionosphere (physics particle precipitation; wave particle interaction) – Magnetospheric physics (storms and substorms)

1 Introduction

Electron fluxes precipitating into the auroral region often show a variety of time structures. The temporal scale of the variations is from fractions of a second to several hundred seconds. Most published studies of the nature of impulsive electron bursts and electron-flux pulsations have suggested explanations based on the theory of whistler cyclotron instability (Coroniti and Kennel, 1970; Davidson and Chiu, 1986;

Trakhtengerts et al., 1986; Demekhov and Trakhtengerts, 1994; Demekhov et al., 1998; Manninen et al., 1996).

The properties of non-stationary regimes of whistler cyclotron instability which exist in the presence of a constant free energy source (e.g. injection of energetic electrons or local acceleration mechanisms) were investigated by Trakhtengerts et al. (1986), Demekhov and Trakhtengerts (1994), Demekhov et al. (1998). A self-exciting model of a whistler cyclotron maser derived from the full set of quasi-linear equations, valid for weak-to-moderate pitch angle diffusion, was developed by these authors to explain certain types of impulsive energetic electron precipitation and auroral electron precipitation pulsations. These types of precipitation have periods of several tens of seconds and are observed in situations where magnetic field variations with the time scales of interest are absent in the equatorial region of the magnetosphere.

On the other hand, a global magnetic field compression caused by large amplitude variations in the solar wind dynamic pressure is believed to be an ideal external mechanism for generating the whistler cyclotron instability (Hayashi et al., 1968; Perona, 1972; Gail et al., 1990). Magnetic field variations in the equatorial magnetosphere directly associated with solar wind dynamic pressure changes are often observed by instruments on geosynchronous satellites (Nopper et al., 1982; Laakso and Schmidt, 1989; Potemra et al., 1989; Wilken et al., 1982; Wilken et al., 1986; Erlandson et al., 1991; Thorolfsson et al., 2001). It is clear that a sharp magnetic field compression which accelerates and flattens the pitch angle of every particle makes the tail of electron distribution, which satisfies the cyclotron resonance condition, unstable to whistler mode emission. A linear change in the wave growth rate leads to an exponential change in the whistler amplitude and therefore in the pitch-angle diffusion rate. Due to wave-particle interaction, the electron's first adiabatic invariant is violated, even though compression alone would conserve it, and precipitation increases. Quasi-linear models based on the theory of gyro-resonance interactions (Kennel and Petchek, 1966) in which a small time-dependent

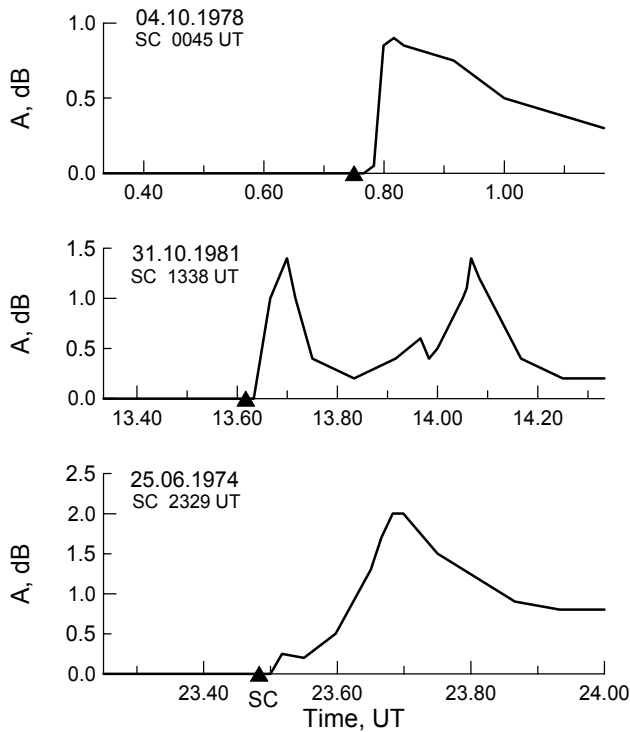


Fig. 1a. Cosmic noise absorption bursts (SCA) caused by solar wind shocks in different local time sectors. Planetary magnetic activity preceding the SC events is low (4 October 1978 – $K_p=2-$; 31 October 1981 – $K_p=1-$; 25 June 1974 – $K_p=1+$). The time of the SC is indicated by the black triangle.

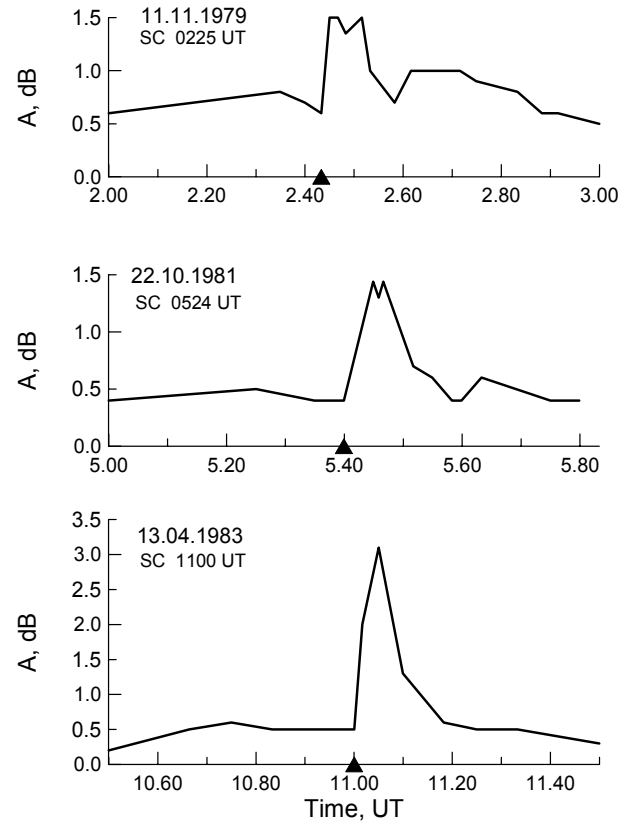


Fig. 1b. Cosmic noise absorption bursts (SCA) caused by solar wind shocks in different local time sectors. Planetary magnetic activity preceding the SC events is high (11 November 1979 – $K_p=3-$; 22 October 1981 – $K_p=4-$; 13 April 1983 – $K_p=3$). The time of the SC is indicated by the black triangle.

perturbation is introduced into the magnetic field, have been derived by Coroniti and Kennel (1970) and Perona (1972) and used to investigate temporal changes in the wave growth rate and diffusion coefficient. Both models take into account adiabatic changes in the pitch-angle anisotropy index A . However, the fraction of the distribution in resonance, η , is assumed to be constant.

Impulsive bursts of VLF emissions associated with the sudden commencement (SC) of geomagnetic storms or with sudden impulses (SI) have been observed by satellites (Kokubun, 1983; Gail and Inan, 1990) at L -shells in the range of $3 < L < 6$ and at ground-based stations at auroral and sub-auroral latitudes (Morozumi, 1965; Hayashi et al., 1968; Kleimenova and Osepian, 1982; Gail et al., 1990; Yahnin et al., 1995; Manninen et al., 1996). Gail et al. (1990) reported that changes in VLF wave activity at high-latitude stations were observed in 50–60% of the events studied and for 80% of the events when the observing station was on the day or morning side of the Earth. Spacecraft data have shown that wave growth is observed on the nightside as well as the day-side, and no clear local time dependence was found (Gail and Inan, 1990). As shown by Gail et al. (1990) the ability of the model suggested by Perona (1972) to predict the observed changes in the properties of diffuse emissions during SCs (growth rate, growth time and total growth) is quite reasonable.

First observations of the SC effect in ionospheric absorption were described by Brown et al. (1961). Ortner et al. (1962) reported that ionospheric absorption during SCs was located around the maximum of the auroral zone and was rarely observed at sub-auroral geomagnetic latitudes. Kleimenova and Osepian (1982) and Gail et al. (1990) observed cases of simultaneous bursts in VLF emissions and ionospheric absorption associated with SC events. Increased electron density at altitudes 80–100 km has also been detected by the EISCAT incoherent-scatter radar during several SC events (Yahnin et al., 1995; Manninen et al., 1996).

In this study we examine impulsive bursts of cosmic noise absorption (SCA) observed at the time of storm sudden commencements (SC) and relate their occurrence and associated absorption values with the perturbation in magnetic field strength, ΔB in the equatorial magnetosphere. We then examine whether these observations can be adequately explained by the whistler cyclotron instability theory. We obtain estimates of the magnitude of ΔB using both measurements of solar wind parameters (with the spacecrafts IMP-8 and Wind) and ground-based measurements of the SC-amplitude ΔH near the equator. A comparison of these two methods can be found in Table 1 with further explanation

Table 1. Dates, times (UT and LT), magnitudes (ΔH , ΔB and ΔA) and background magnetic activity (K_p) for a representative subset of the events analysed.

Date	UT	LT	ΔH nT	ΔB $L=5.3$	ΔB IMP-8	K_p	ΔA dB
23 June 1974	08:57	13:49	22	20	26	1	0.0
4 July 1974	15:34	20:26	31	16	19	4	0.8
21 September 1974	12:46	17:32	22	15	17	4-	1.1
12 October 1974	12:44	17:36	26	19	22	2-	0.0
18 January 1977	04:22	09:14	13	11	8	1+	0.0
25 November 1977	12:24	17:16	26	19	22	1	0.0
3 January 1978	20:42	01:34	23	11	9.5	3	0.4
13 April 1978	19:24	00:16	24	10	9.0	3	1.0
17 April 1978	23:44	04:36	15	9.0	10	1	0.0
21 May 1978	02:40	07:32	21	15	10	1+	0.0
4 June 1978	12:11	17:03	23	17	17	3-	0.4
18 August 1978	12:41	17:33	17	11	14	1+	0.0
21 February 1979	03:00	07:52	17	14	15	2+	0.4
6 June 1979	19:27	00:19	80	36	34	3	1.0
12 July 1979	12:39	17:31	11	8.5	13	1	0.0
26 July 1979	18:33	23:25	27	12	8.5	2	0.6
29 August 1979	04:59	09:51	23	18	15	3	1.8
25 January 1980	11:08	16:00	13	11	13	1-	0.0
19 March 1980	06:18	11:10	34	31	33	1-	0.4
7 May 1980	08:03	12:55	19	17	19	1-	0.0
29 May 1980	18:33	23:25	13	5	7	1+	0.0
18 July 1980	19:25	00:17	48	21	24	3-	0.3
6 February 1981	08:48	13:40	12	11	14	2+	0.4
10 May 1981	22:08	03:08	40	20	16	4+	1.6
30 August 1981	22:21	03:13	19	9.6	10	1+	0.0
22 October 1981	05:24	10:16	35	29	23	4-	1.0
12 June 1982	14:42	19:34	37	22	27	3-	0.5
13 July 1982	16:17	21:09	87	43	38	4+	1.4
13 April 1983	11:00	15:52	45	36	50	3	1.1
24 May 1983	12:39	17:31	25	17	15	3-	0.6
4 October 1983	05:42	10:34	15	13	12	3	0.6
20 February 1984	15:50	20:42	22	11	7	2-	0.0
9 July 1984	16:38	21:30	14	7	9	2+	0.0
11 September 1986	18:35	23:27	32	14	16	1-	0.0
4 April 1987	03:13	08:05	39	32	40	1-	0.8
24 July 1987	16:33	21:25	29	14	13	2-	0.0
24 September 1987	01:54	06:46	24	17	21	1-	0.0
4 January 1988	20:09	01:01	37	16	13	2-	0.0
12 February 1988	21:24	02:16	28	13	16	3+	1.1
25 August 1988	09:33	14:25	26	22	23	3	0.6
10 October 1988	02:31	07:23	18	14	18	3+	0.4
30 October 1988	20:00	00:52	25	12	17	0+	0.0
16 March 1989	05:30	10:22	50	43	40	2-	0.9
11 April 1989	14:35	19:27	29	16	19	1+	0.0
7 May 1989	05:12	10:04	71	58	46	1-	1.0
23 May 1989	13:46	18:38	68	41	39	2-	0.8
13 June 1989	17:39	22:31	26	12	13	1+	0.0
14 August 1989	06:12	11:04	70	59	50	4	1.7
27 August 1989	13:36	18:28	32	21	23	3-	0.6
22 September 1989	07:39	12:31	24	21	30	3	1.1
26 November 1989	10:53	15:45	23	18	22	1+	0.0
28 November 1989	07:42	12:34	32	28	22	4+	1.4
29 December 1989	06:55	11:47	28	25	23	2	0.4

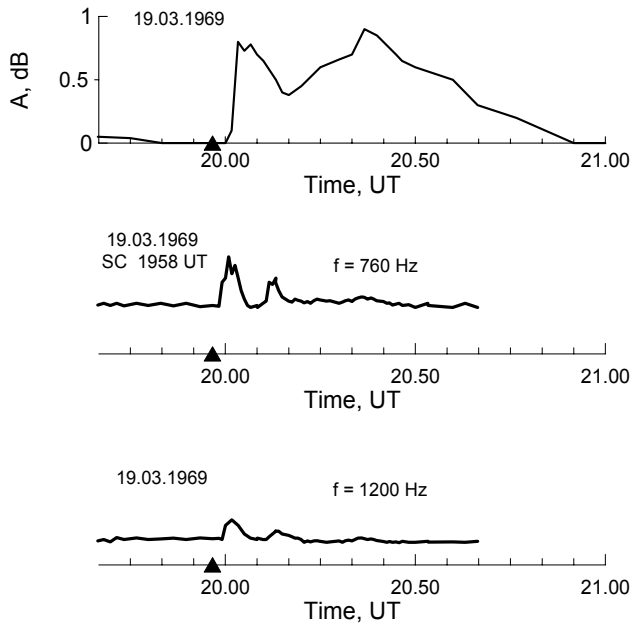


Fig. 2a. Cosmic noise absorption (SCA) and bursts of VLF-emission observed on 19 March 1969. Planetary magnetic activity preceding the SC event is low ($K_p=1+$). The time of the SC is indicated by the black triangle.

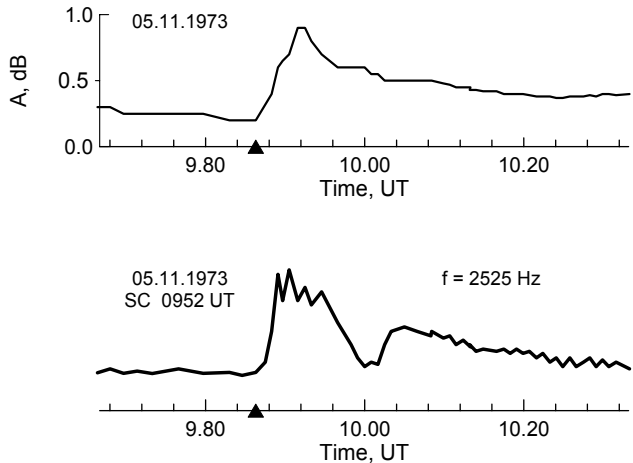


Fig. 2b. Cosmic noise absorption (SCA) and burst of VLF-emission observed on 5 November 1973. Planetary magnetic activity preceding the SC event is high ($K_p=3$). The time of the SC is indicated by the black triangle.

in the Appendix. In Sect. 2 we show that the SC effect in ionospheric absorption depends on the pre-history or the state of the magnetosphere before the SC event. In Sects. 3 and 4 we investigate temporal changes in the anisotropy index, the wave growth rate and the pitch-angle diffusion caused by a perturbation ΔB . We use the approach to this problem described by Coroniti and Kennel (1970) and Perona (1972). We take into account changes in all parameters included in the equation for wave growth, including changes in the fraction of resonant electrons, η , due to adiabatic changes and

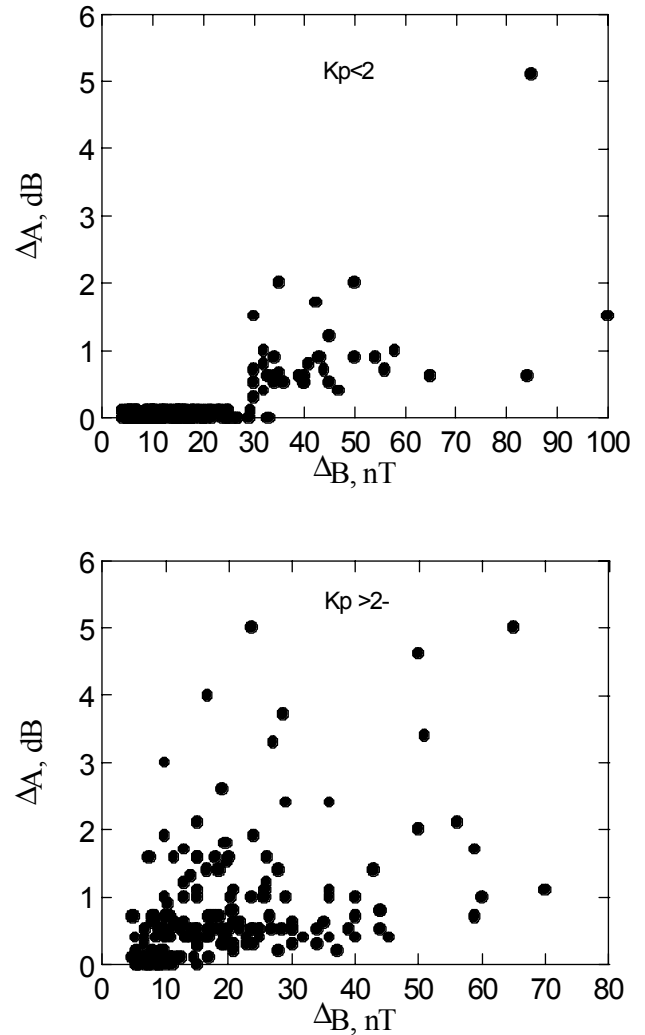


Fig. 3. Magnitude of the impulse in cosmic noise absorption ΔA as a function of the magnetic impulse ΔB induced by the SC at the magnetic equator at $L=5.3$. The upper panel is for quiet conditions ($K_p < 2$) preceding the SC, the lower panel is for active conditions ($K_p \geq 2$).

acceleration of hot particles in the induction electric field. In Sect. 3 we estimate the time delay of absorption bursts relative to the magnetic impulse associated with the SC for SC events observed against a quiet background ($K_p < 2$). We also estimate the value of perturbation ΔB in the magnetic field strength required to generate whistler cyclotron instability against a background corresponding to a quiet magnetosphere. In Sect. 4 we determine relative changes in pitch-angle diffusion coefficient D^* caused by SC events observed against an active background ($K_p \geq 2$) and predict changes in absorption value during real SC events.

2 Experimental data

Variations of cosmic radio-noise absorption at times of sudden commencements (SC) of geomagnetic storms are studied

using riometer records obtained at the station Loparskaya ($\Phi=64^\circ$ N, $\Lambda=115.5^\circ$ E, $L=5.3$) for the period 1967–1990. We excluded from consideration all cases when the SC was observed against a background of solar proton precipitation (solar proton events, SPE). As a result, 352 of the SC events registered by magnetic stations for 1967–1990 are included in our study. We find that the response of cosmic radio-noise absorption to the passage of the bow shock depends on the level of the planetary magnetic activity (K_p index) preceding the SC. From the 352 SC events considered, only 190 cases are accompanied by bursts of SCA. For 174 SC events observed against a quiet background ($K_p < 2$), effects of the SC are seen in absorption only for 33 cases (18.9%). For 178 SC events observed against an active background ($K_p \geq 2$) bursts in absorption are observed on 157 occasions (88.2%). Examples of SCA bays during SC observed against backgrounds of both low and high activity are shown in Figs. 1a, b.

Figure 2a shows records of SCA in Loparskaya and VLF bursts observed in Sogra ($\Phi'=56.6^\circ$ N, $\Lambda=124^\circ$ E, $L=3.7$) at the time of the SC on 19 March 1969 at 19:58 UT (planetary magnetic activity before the SC is low, $K_p=1+$). Figure 2b presents SCA in Loparskaya and VLF emission observed in Lovozero ($\Phi'=63.8^\circ$ N, $\Lambda=127^\circ$ E, $L=5.1$) at the time of the SC on 5 November 1973 at 09:52 UT ($K_p=3$ preceding the SC in this case). It can be seen that for the SC observed against a quiet background (Figs. 1a, 2a), there is a short (about 30–60 s) delay of the SCA bay and VLF burst relative to the SC. In active periods, absorption and VLF emission increase together with the SC (Figs. 1b, 2b). Figure 3 shows the relationship between the magnitude of absorption bursts and of the magnetic impulse ΔB induced by the SC in the equatorial magnetosphere at $L=5.3$. The upper panel is for quiet conditions ($K_p < 2$) preceding the SC; the lower panel is for active conditions ($K_p \geq 2$). The method of determining ΔB is described in the Appendix. It is clear that in the quiet case absorption bursts are observed only when the perturbation ΔB exceeds a threshold value $\Delta B_{th} \approx 30$ nT. In the disturbed case almost all SC events, including very small perturbations, are accompanied by bursts in absorption.

3 Magnetic field perturbation ΔB needed to excite whistler cyclotron waves at $L=5.3$

In this section we show that properties of absorption bursts (SCA), such as the dependence of occurrence on K_p preceding the SC event, the threshold value ΔB_{th} and the time delay of SCA relative to the SC, can be predicted in the context of the whistler cyclotron instability theory.

We first give a brief review of the whistler cyclotron instability theory. Growth and damping of whistler mode waves with frequency ω are controlled by the characteristics of the ambient magnetospheric plasma (hot and cold plasma density, pitch-angle distribution function, fraction of resonant electrons) which change depending on the level of planetary magnetic activity. It is generally expected that pre-conditions

must be satisfied in order to produce wave growth. The temporal growth rate γ of whistler waves at frequency ω derived by Kennel and Petschek (1966) is

$$\gamma = \pi \Omega_e \eta(E_{res}) \{A^-(E_{res}) - 1/[(\Omega_e/\omega) - 1]\} \{1 - (\omega/\Omega_e)\}^2, \quad (1)$$

where Ω_e is the electron gyrofrequency; $E_{res} = m_e V_{res}^2/2$ is the parallel electron energy required for Doppler-shifted cyclotron resonance with whistler mode waves at frequency ω , m_e is the electron mass; B_0 is the magnetic field in the equatorial plane, $A^-(E_{res})$ is the index of electron pitch-angle anisotropy $\eta(E_{res})$ is the fraction of the total particle distribution which satisfies the resonance condition (its exact definition is given by Kennel and Petschek, 1966). $\eta(E_{res})$ is related to the omnidirectional flux $J_{2\pi}(E \geq E_{res})$, which is an observed quantity, by the following relation:

$$\eta(E_{res}) = J_{2\pi}(E \geq E_{res}) / 2V_{res}N \quad (1a)$$

where N is the cold plasma density.

Since $\eta(V_{res})$ is always positive, the wave grows ($\gamma > 0$) if the anisotropy $A^-(E_{res})$ is greater than a critical value A_c^- which is frequency dependent

$$A^-(E_{res})_c = \{(\Omega_e/\omega) - 1\}^{-1}. \quad (1b)$$

The maximum initial frequency ω_{mo} of unstable ($\gamma \geq 0$) cyclotron waves is determined by the following inequality

$$\omega_{mo} < A_0^- \Omega_e / (1 + A_0^-) \ll \Omega_e, \quad (2)$$

where A_0^- is a initial anisotropy.

For instability to be self-sustaining, the total amplification of whistler waves on one pass between conjugate ionospheres must compensate the wave losses due to reflection at the magnetosphere-ionosphere interface. Mathematically, the condition required to maintain self-exciting waves is presented in the following form (Cornilleau-Wehrin et al., 1985; Demekhov and Trakhtengerts, 1994):

$$\Gamma = \int \gamma dS / V_g \geq |\ln 1/R| \quad \text{or} \quad \gamma \geq \gamma_{th} = \nu \equiv (V_g/LR_e) |\ln R|, \quad (3)$$

where ν is the loss rate of the wave energy, R is the effective reflection coefficient from the ionosphere. The reflection coefficient R is difficult to evaluate. As a rule, the numerical value $|\ln 1/R|$ is assumed to be equal to 3 (Cornilleau-Wehrin et al., 1985; Schulz and Davidson, 1988). $V_g = 2B_0/(4\pi m_e N)^{1/2} (\omega/\Omega_e)^{1/2} (1 - \omega/\Omega_e)^{3/2}$ is the equatorial group velocity of the wave at a given L -shell; dS is the increment of the magnetic field line length; $l \approx LR_E$ is the resonator length between the reflection points on the given magnetic field line; R_E is the radius of the Earth.

The condition (3) is satisfied in that region of the magnetosphere where the temporal growth rate is positive and there are enough electrons near resonance, i.e. the total flux of trapped electrons $J(E \geq E_{res})$ exceeds the threshold value $J^*(E \geq E_{res}) \approx 1 \times 10^{11} / L^4$ (Kennel and Petschek, 1966;

Table 2. Calculated parameters of whistler wave growth at various levels of planetary magnetic activity (K_p). Plasma density (N) and flux of energetic electrons (J) are assumed parameters. The calculated parameters are temporal growth rate (γ), spatial growth rate (γ/V_g), loss rate (ν) and the minimum jump in magnetic field (ΔB) needed to raise the growth-rate to the level where it exceeds the critical value estimated by Cornilleuau-Werlin et al. (1985)(all calculations for $L=5.3$, $\omega/\Omega_e=0.12$, $A_0^-=0.3$, $\ln(1/R)=3$).

K_p	N cm^{-3}	$J(E>E_{Res})$ $\text{cm}^{-2}\text{s}^{-1}$	ν, s^{-1}	γ, s^{-1}	γ/ν	γ/V_g	$\Delta B, \text{nT}$
0	100	$(1-2)\times 10^7$	1.08	0.16–0.32	0.14–0.29	$(1.3-2.6)\times 10^{-10}$	80–55
	50	$(1-2)\times 10^7$	1.53	0.22–0.45	0.14–0.29	$(1.3-2.6)\times 10^{-10}$	80–55
	10	$(1-2)\times 10^7$	3.41	0.49–0.99	0.14–0.29	$(1.3-2.6)\times 10^{-10}$	80–55
0–1	100	$(2-3)\times 10^7$	1.08	0.32–0.47	0.29–0.44	$(2.6-4.0)\times 10^{-10}$	55–35
	50	$(2-3)\times 10^7$	1.53	0.45–0.67	0.29–0.44	$(2.6-4.0)\times 10^{-10}$	55–35
	10	$(2-3)\times 10^7$	3.41	0.99–1.50	0.29–0.44	$(2.6-4.0)\times 10^{-10}$	55–35
1	10	$(2.5-4)\times 10^7$	3.41	1.25–2.0	0.36–0.58	$(3.3-5.2)\times 10^{-10}$	40–25
	5	$(2.5-4)\times 10^7$	4.83	1.76–2.8	0.36–0.58	$(3.3-5.2)\times 10^{-10}$	40–25
≥ 2	10	$(5-7)\times 10^7$	3.41	2.49–3.49	0.73–1.02	$(6.5-9.3)\times 10^{-10}$	10–0
	5	$(5-7)\times 10^7$	4.83	3.53–4.94	0.73–1.02	$(6.5-9.3)\times 10^{-10}$	10–0
Bulge region							
0–1	100	$(2-3)\times 10^7$	1.08	0.32–0.47	0.29–0.44	$(2.6-4.0)\times 10^{-10}$	55–35
	50	$(2-3)\times 10^7$	1.53	0.22–0.67	0.29–0.44	$(2.6-4.0)\times 10^{-10}$	55–35
1	100	$(2.5-4)\times 10^7$	1.08	0.39–0.63	0.36–0.58	$(3.3-5.2)\times 10^{-10}$	40–25
	50	$(2.5-4)\times 10^7$	1.53	0.55–0.89	0.36–0.58	$(3.3-5.2)\times 10^{-10}$	40–25
1–2	100	$(5-7)\times 10^7$	1.08	0.79–1.10	0.73–1.02	$(6.5-9.3)\times 10^{-10}$	10–0
	50	$(5-7)\times 10^7$	1.53	1.12–1.56	0.73–1.02	$(6.5-9.3)\times 10^{-10}$	10–0
	10	$(5-7)\times 10^7$	3.41	2.49–3.49	0.73–1.02	$(6.5-9.3)\times 10^{-10}$	10–0
≥ 2	10	$(6-7)\times 10^7$	3.41	3.00–3.49	0.88–1.02	$(7.9-9.3)\times 10^{-10}$	5–0
	5	$(6-7)\times 10^7$	4.83	4.23–4.94	0.88–1.02	$(7.9-9.3)\times 10^{-10}$	5–0

Schulz and Davidson, 1988). A critical value for the spatial growth rate γ/V_g is estimated to be $\gamma_{th}/V_g \approx 1 \times 10^{-9} \text{ cm}^{-1}$ (Cornilleuau-Wehrin et al., 1985).

In Table 2 we present quantitative evaluations of the temporal (γ) and spatial (γ/V_g) growth rates and the loss rate (ν) calculated for the equatorial plane at $L=5.3$ for different levels of planetary magnetic activity. We assume that reduced resonant frequency $x=\omega/\Omega_e=0.12-0.15$, magnitude of anisotropy index $A^-(E_{Res})=0.3$ and resonant energy $E_{Res}=30 \text{ keV}$ are the most realistic plasma parameters in the equatorial magnetosphere at $L=5-6$ (Cornilleuau-Wehrin et al., 1985; Kirkwood and Osepian, 2001).

We also need to use realistic values of the cold plasma density (N) and trapped electron fluxes $J(E \geq 30 \text{ keV})$. Large numbers of measurements have been obtained with satellites near the equatorial plane at $L=5.0-5.5$. It is well established that there is a region of sharp gradient in the distribution of the cold plasma density in the magnetosphere – the plasmapause – where the plasma density decreases by 1–2 orders of magnitude. The location of the plasmapause, L_P , depends on the level of magnetic activity and on the MLT sector (Carpenter, 1967; Binsak, 1967; Chap-

pel et al., 1970a; Chappel et al., 1970b; Harris et al., 1970; Rycroft and Thomas, 1970; Chappel et al., 1971; Park et al., 1978; Singh and Horwitz, 1992). As a rule, the L -shell $=5.3$ is located outside the plasmasphere ($L_P < 5.3$) if the K_p index is about 1 or higher. In these cases we take values $N=10-5 \text{ cm}^{-3}$ to evaluate the increment, the loss rate and the spatial (γ/V_g) growth rate of the wave, (Harris et al., 1970; Chappel et al., 1971; Carpenter and Chappel, 1973; Morgan and Maynard, 1976). For $K_p=0-1-$, we take $N=100-50 \text{ cm}^{-3}$ if $L_P > 5.3$ and $N=10-5 \text{ cm}^{-3}$ if $L_g < 5.3$. In the bulge region of the plasmasphere (18:00–21:00 MLT) the L -shell $=5.3$ is located outside the plasmasphere for $K_p > 2$. In this LT-region we use values of $N=100-50 \text{ cm}^{-3}$ for $K_p=0-2$ and $N=10-5 \text{ cm}^{-3}$ for $K_p \geq 2$ (Chappel et al., 1970b; Carpenter and Chappel, 1973; Morgan and Maynard, 1976; Singh and Horwitz, 1992).

Similarly, there are many observations made of the trapped electron fluxes with $E > 10-40 \text{ keV}$ near the equatorial plane of the magnetosphere. We have examined data obtained with satellites of the series ATS, OGO, Explorer 12 and 45 and GEOS. In Table 2 we use typical values of the trapped electron fluxes $J(E \geq 30 \text{ keV})$ observed at $L=5.0-5.5$ during

both low and high planetary magnetic activity (Kivelson et al., 1973; West et al., 1973; Lyons and Williams, 1975; Collis et al., 1983; Davidson et al., 1988; Reeves, 1994).

Note that for our chosen parameters $A^-(E_{res})$, ω/Ω_e , $|\ln 1/R|=3$ and values N and $J(E \geq 30 \text{ keV})$ indicated in Table 2, the spatial growth rate reaches the critical value $(\gamma_{th}/V_g) \approx 1 \times 10^{-9} \text{ cm}^{-1}$ when the trapped electron flux $J(E \geq 30 \text{ keV})$ is about $7 \times 10^7 \text{ (cm}^{-2}\text{s}^{-1})$ which is close to the limiting flux $J^*(E \geq E_{res})$ predicted by the theory. This occurs only in the disturbed magnetosphere when K_p is approximately equal to or greater than 2. In contrast, under conditions where initial fluxes of trapped electrons $J(E \geq 30 \text{ keV})$ at $L=5.3$ are small (i.e. where $K_p < 2$) the ratio $\gamma/\nu < 1$ and $\gamma/V_g < 1 \times 10^{-9} \text{ cm}^{-1}$, i.e. growth will not occur.

To determine the SC amplitude, ΔB , needed to excite whistler cyclotron waves, we derive an equation describing temporal changes in the wave growth rate during an SC observed against a background of low planetary magnetic activity. According to Perona (1972), the time-dependent magnetic field perturbation in the equatorial magnetosphere can be written in the form:

$$B = B_0(1 + bt), \quad (4)$$

where B_0 is the initial value of the magnetic field at a given L -shell and the parameter b is chosen in such a way ($b = \Delta B/B_0 T$) that, at the end of the event, namely, at $t=T$, the value of the magnetic field reaches its final value $B(T)$; T is the duration of the SC event. Taking into account possible changes in all parameters (B , A^- and η) in the equation for the wave growth rate (1) we can write:

$$\frac{d \ln \gamma}{dt} = \frac{d \ln B}{dt} + \frac{d \ln A^-}{dt} + \frac{d \ln \eta}{dt}.$$

In the region with energy $E \geq 10 \text{ keV}$ the initial equilibrium velocity distribution function can generally be assumed to have a bi-Maxwellian form with the anisotropy index

$$A^- = \frac{(T_{\perp} - T_{\parallel})}{T_{\parallel}}, \quad (5)$$

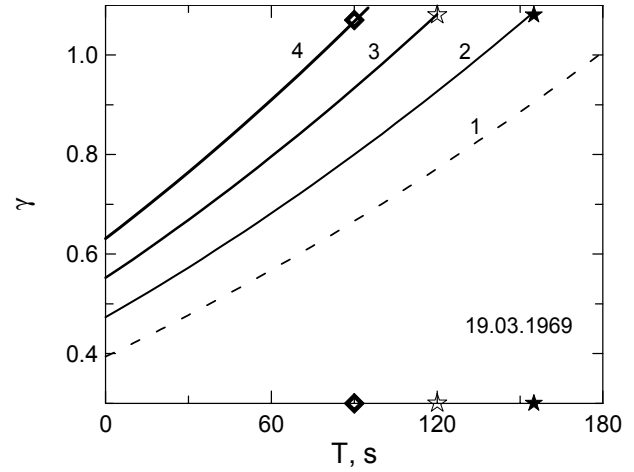
where T_{\perp} and T_{\parallel} are average temperatures of energetic electrons normal and parallel to the magnetic field line. On the condition that the first adiabatic invariant is conserved, for example, T_{\perp} is proportional to $B(t)$, an equation describing the change in the anisotropy during the SC caused by compression alone can be written as (Coroniti and Kennel, 1970):

$$\frac{d \ln A^-}{dt} = \frac{\partial \ln A^-}{\partial B} \frac{dB}{dt} = \frac{(1 + A^-)}{A^-} \frac{b}{(1 + bt)}. \quad (6)$$

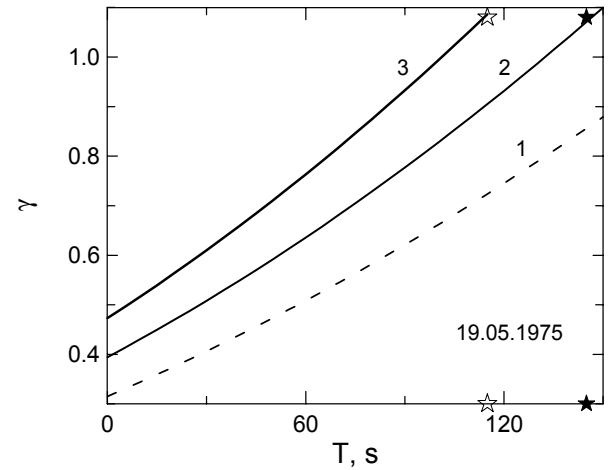
Recalling that η is related to the total flux of trapped electrons by Eq. (1a) and $E_{Res} \sim E_c = B_0^2/8\pi N$ variations in η can be written as

$$\frac{d \ln \eta}{dt} = \frac{d \ln J}{dt} - \frac{d \ln V_{Res}}{dt} - \frac{d \ln N}{dt}.$$

Induced electric field \mathbf{E}^* ($\text{rot } \mathbf{E}^* = -1/c(\partial \mathbf{B}/\partial t)$) produced by the abrupt compression of the magnetosphere increases



- 1 - $J(>30 \text{ keV}) = 2.5e7$; 2 - $J(>30 \text{ keV}) = 3.0e7$;
3 - $J(>30 \text{ keV}) = 3.5e7$; 4 - $J(>30 \text{ keV}) = 4.0e7$.



- 1 - $J(>30 \text{ keV}) = 2.0e7$; 2 - $J(>30 \text{ keV}) = 2.5e7$;
3 - $J(>30 \text{ keV}) = 3.0e7$.

Fig. 4. Change of the temporal growth rate of whistler waves during two SC events. Planetary magnetic activity preceding the SC events is low ($K_p=1+$ and 0). The different curves correspond to different assumptions of the initial flux of trapped electrons at energies $E \geq 30 \text{ keV}$ for the given values of K_p . The symbols show when the wave increment reaches the generation threshold.

the kinetic energy of trapped electrons. The change in kinetic energy per unit time during the SC is written as (Osepián, 1973; Mal'tzev, 1998):

$$\frac{dE}{dt} = \frac{5}{2} - E \frac{1}{B} - \frac{dB}{dt}.$$

Then taking into account betatron acceleration, the frozen-in flux condition and assuming that the energetic spectrum of trapped electrons with $E \geq 30 \text{ keV}$ is described by an exponential ($dj/dE = j_0 \exp(-E_{res}/E_0)$) function we obtain

$$\frac{d \ln \eta}{dt} \approx \frac{5}{2} - \frac{b}{1 + bt}.$$

Then the differential equation describing the change in the wave growth rate during SC events observed against a quiet background ($K_p < 2$) can be written in the form:

$$\frac{d\gamma}{dt} = \frac{3.5b}{1+bt}\gamma + \frac{1}{A^-} \frac{b}{1+bt}\gamma. \quad (7)$$

Figure 4 shows calculations of how quickly the wave growth rate increases to the wave-generation threshold at times of two real SC events which were accompanied by VLF and absorption bursts. The first case is the SC event observed at 19:58 UT on 19 March 1969 (Fig. 2a). The amplitude of SC ΔB is 40 nT, $T=180$ s, $K_p=1+$. The second case is the SC observed at 19:51 UT on 19 May 1975. Here $\Delta B=45$ nT, $T=150$ s, $K_p=0+$. The different curves correspond to different assumptions of the initial flux of trapped electrons at energies $E \geq 30$ keV. Initial values γ_0 are taken from Table 2 (column 3). The symbols show when the wave growth rate reaches the generation threshold. The minimum delay time is about 90–110 s. Note that delays of 1–2 min between SC and absorption bursts can be discerned in Figs. 1a and 2a. Note also that even quite large SC amplitudes would not lead to whistler wave generation (curves 1) if the SC events occurred against a completely quiet background ($K_p=0$).

In Table 2, in the last column, we present the minimum magnitude of the magnetic field jump, ΔB , which would cause an increase of spatial wave growth rate γ/V_g to the threshold magnitude γ_{th}/V_g for different pre-conditions in the magnetosphere. To calculate these values, solutions of the differential Eq. (7) were obtained for different initial values γ_0 corresponding to initial values of trapped flux at the given K_p . The SC rise time is taken to be equal $T=180$ s. It is seen that in the absolutely quiet magnetosphere ($K_p=0$) very large SC amplitudes ($\Delta B=80$ – 55 nT) are required to excite the whistler cyclotron instability at $L = 5.3$. For K_p in the range 1+ to 2-, the minimum magnitude ΔB needed is 25 nT. These results are quantitatively consistent with our experimental data which indicate a threshold magnitude ΔB about 30 nT (Fig. 3).

4 Calculation of diffusion coefficients and cosmic radio-noise absorption during SC events using the whistler cyclotron instability theory

Values of temporal γ and spatial γ/V_g growth rates presented in Table 2 show that when initial fluxes of trapped electrons $J(E \geq 30$ keV) at $L=5.3$ are large enough (for $K_p \geq 2$), the ambient electron distribution is unstable or nearly unstable to whistler mode waves. A quasi-equilibrium state, where there is a balance between sources and sinks of particles and waves, may exist before the SC events, keeping the growth rate of whistler waves near or slightly above the level of marginal stability ($\gamma \approx \nu$). This implies that riometers can measure significant background absorption preceding SC events, as is seen in Figs. 1b and 2b. In this case, even a small external perturbation ΔB can result in positive wave growth rate, enhancement of pitch-angle diffusion and

absorption bursts during the SC, as is seen in Figs. 1b, 2b and 3. When a quasi-equilibrium state between waves and particles is present at the initial moment t_0 and the relaxation time T_{Rel} of the system to a new a diffusion equilibrium configuration is small compared to the duration of the SC ($T_{Rel} < T$) it is possible to evaluate the relative change in the diffusion coefficient $D^*(T)/D^*(t_0)$ caused by the SC.

In this section we apply the quasi-linear theory of whistler instability to evaluate changes in the pitch-angle diffusion coefficient D^* at the edge of the loss cone and to calculate absorption $A(T)$ caused by a magnetic field perturbation ΔB . We resolve a set of three coupled differential equations describing the change in anisotropy index, temporal growth rate and diffusion coefficient due to both compression and diffusion processes taking place during the SC.

Simple analytical expressions for anisotropy are given by the theory only for the limits of weak and strong diffusion (Kennel and Petschek, 1966; Etcheto et al., 1973). In the regime of very weak diffusion the anisotropy A^- is independent of the diffusion coefficient $A^- = 1/2 \ln(1/\alpha_0)$. In the regime of strong diffusion $A^- = \alpha_o^2/4D^*T$. For an arbitrary diffusion strength $A^- \sim 1/D^{*\beta}$ and the relation between A^- and D^* can be written in the following form (Haugstad, 1975; Kirkwood and Osepian, 2001):

$$A^-(t) = A^-(t_0) \times (D^*(t_0)/D^*(t))^\beta,$$

where β varies from $\beta=0$ to $\beta=1$, depending on the diffusion regime assumed during the SC; $D^*(t_0)$ is an initial value of the diffusion coefficient; preceding the SC; $A^-(t_0)$ is an initial anisotropy index given by Eq. (5). Then the change in anisotropy during the SC is described by the equation:

$$\frac{d \ln A^-}{dt} = \frac{(1 + A^-)}{A^-} \frac{b}{(1 + bt)} - \beta \frac{d \ln D^*}{dt}. \quad (8)$$

Finally, the differential Eq. (7), describing the change in the wave increment γ in response to changes in B , η and A^- , is reduced to:

$$\frac{d\gamma}{dt} = \frac{3.5b}{1+bt}\gamma + \frac{1}{A^-} \frac{b}{1+bt}\gamma - \beta\gamma \frac{1}{D^*} \frac{dD^*}{dt}. \quad (9)$$

Since the diffusion coefficient due to whistler-particle interaction is proportional to the square of the wave amplitude, the equation for the diffusion coefficient is written as (Coroniti and Kennel, 1970)

$$\frac{dD^*}{dt} = 2(\gamma(t) - \gamma(t_0))D^*. \quad (10)$$

The coupled set of differential Eqs. (8–10) have been resolved for different values $\beta=0$ – 1 , magnitudes $\Delta B=5$ – 40 nT and $T=120$ – 360 s. Calculations have been made for L -shells 5.3, 6.0 and 6.6. Figure 5 shows changes in anisotropy index A^- , wave increment γ and diffusion coefficient D^* at the equatorial plane ($L=5.3$) caused by a magnetic field perturbation $\Delta B=40$ nT with duration $T=180$ s. The initial wave growth rate $\gamma(t_0)$ is assumed to be equal to the wave loss rate ν or threshold value γ_{th} . At $L=5.3$ this value is taken from Table 2 for

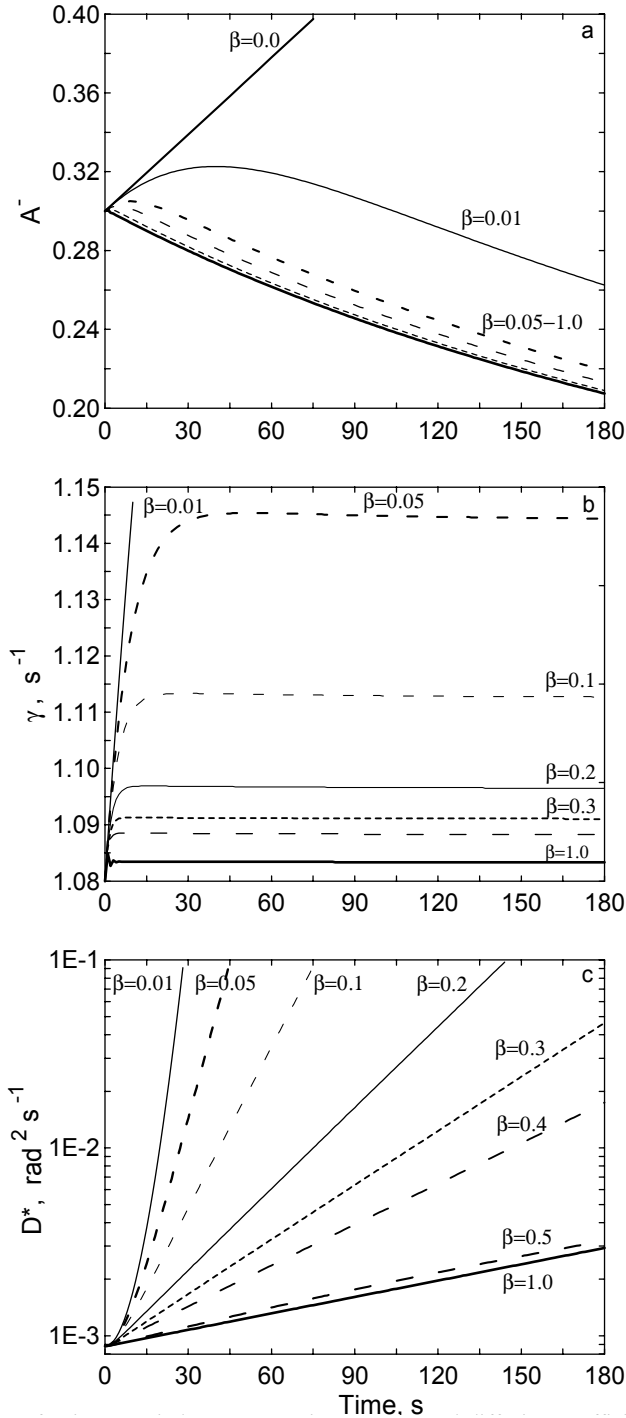


Fig. 5. Changes in anisotropy index A^- , wave increment γ and diffusion coefficient D^* at the equatorial plane ($L=5.3$) caused by magnetic field perturbation $\Delta B=40$ nT with duration $T=180$ s. Parameter β characterizes diffusion strength assumed during the SC.

$K_p=2$. Initial values of the anisotropy index ($A^-(t_0)=0.3$) and diffusion coefficient ($D^*(t_0)=8.8 \times 10^{-4} \text{ rad}^2 \text{ s}^{-1}$) are assumed to be equal to typical values of these parameters for the background equilibrium state at a given L -shell (Kirkwood and Osepian, 2001).

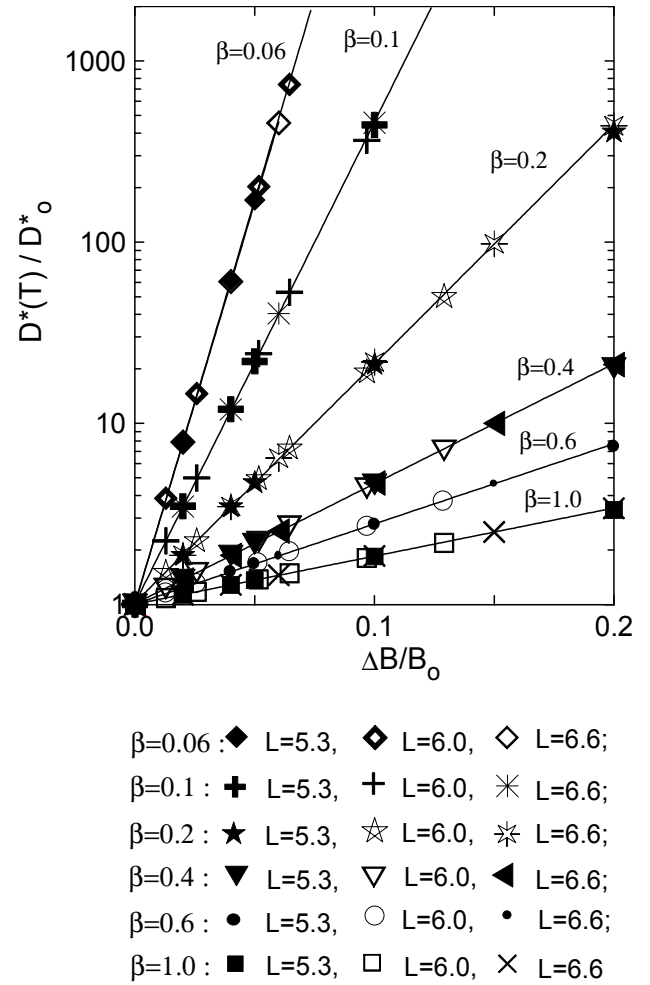


Fig. 6. Magnitude of relative change of diffusion coefficient $D^*(T)/D^*(t_0)$ as a function of $\Delta B/B_0$ obtained for different values of parameter β .

The process of magnetic field compression leads to an unlimited increase in A^- , γ and D^* . As soon as the diffusion process is turned on, anisotropy decreases very quickly and growth of the wave increment and diffusion coefficient is limited. The growth duration of the wave increment is less than the SC rise time. It depends on the diffusion strength (parameter β). In the regime of weak diffusion, energy accumulation by the wave lasts longer than in the regime of strong diffusion. Thus, the wave-particle system reaches a new quasi-equilibrium state in the early phase of the SC with values of $\gamma(t)$ close to but a little above the initial value γ_0 .

Since the relaxation time T_{Rel} (maximum value T_{Rel} is about 30 s) of the system to a new diffusion equilibrium is less than the SC rise time, T , we can determine the magnitude of relative change in diffusion coefficient $D^*(T)/D^*(t_0)$ for different diffusion regimes realised during the SC. As can be seen in Fig. 6, the change in the diffusion coefficient is an exponential function of the magnitude

Table 3. Coefficients a and c in Eq. (11) at the different L -shells found as a result of numerical solution of Eqs. (8–10).

β	$L=6.6$		$L=6.0$		$L=5.3$	
	a	$c=a \times \beta$	a	$c=a \times \beta$	a	$c=a \times \beta$
0.01	594.7	5.95	594.4	5.94	599.2	5.99
0.02	301.1	6.02	300.0	6.00	299.9	5.98
0.03	198.8	5.96	198.3	5.96	199.3	5.98
0.04	149.9	5.99	150.7	6.03	150.64	6.02
0.05	120.65	6.03	120.76	6.04	121.19	6.06
0.06	101.0	6.06	100.70	6.04	101.11	6.06
0.07	86.80	6.08	86.37	6.04	86.88	6.08
0.08	76.12	6.09	75.60	6.05	76.03	6.08
0.09	67.79	6.10	67.22	6.05	67.59	6.08
0.1	61.11	6.11	60.05	6.00	60.08	6.00
0.2	30.40	6.08	30.30	6.06	29.99	5.99
0.3	20.31	6.09	20.19	6.06	19.99	5.99
0.4	15.25	6.10	15.16	6.06	15.00	6.00
0.5	12.21	6.10	12.13	6.06	12.00	6.00
0.6	10.18	6.11	10.10	6.06	10.00	6.00
0.7	8.73	6.11	8.66	6.06	8.57	5.99
0.8	7.64	6.11	7.58	6.06	7.49	5.99
0.9	6.79	6.11	6.73	6.06	6.66	5.99
1.0	6.11	6.11	6.06	6.06	5.99	5.99

$\Delta B/B_0$ at a given L -shell and parameter β :

$$\frac{D^*(T)}{D_0^*} = \exp\left(a \frac{\Delta B}{B_0}\right) = \exp\left(\frac{c}{\beta} \frac{\Delta B}{B_0}\right), \quad (11)$$

where the coefficients a and c ($c=a \times \beta$) have the same values at any L -shell for a given β . They are presented in Table 3. Solutions of Eqs. (8–10) obtained for different values of the SC rise time T show that the maximum change in diffusion coefficient $D^*(T)$ is by a factor 1.2 for the range $T=120-360$ s.

Provided that the wave-particle system is in a quasi-equilibrium state, the total flux of precipitating electrons J_p with $E \geq E_{Res}$ is proportional to the diffusion coefficient and at the time of the SC events we have

$$J_p(T) = J_p(t_0) \exp\left(\frac{c}{\beta} \frac{\Delta B}{B_0}\right).$$

Knowing the magnitude of the field perturbation ΔB in the equatorial magnetosphere at the given L -shell and recalling that absorption A is proportional to $J_p(E \geq E_{Res})^-$, we are able to calculate absorption SCA for real SC events for different diffusion regimes. In Table 4 we compare calculated

values of absorption A_{cal} with A_{exp} measured in Loparskaya to evaluate the ability of the quasi-linear model to describe a number of qualitative and quantitative features of absorption bursts induced by SCs, and to determine the diffusion regime realized during the real SC events. Note that, although all available events have been analysed, we include only a selection of typical examples in Table 4 covering the range of values of ΔB and A_{exp} represented in the full data set.

5 Discussion and Conclusions

We have examined bursts of cosmic noise absorption (SCA) observed during sudden commencements (SC) of geomagnetic storms. We find that the response of cosmic noise absorption to the passage of an interplanetary shock depends on the level of planetary magnetic activity preceding the SC and on the magnitude of the geomagnetic field perturbation Δ induced by the SC at the given L -shell in the equatorial magnetosphere. We have shown that, for SC-events observed against a quiet background ($K_p < 2$), an effect of the SC on absorption can be seen only when ΔB caused by the solar

wind shock exceeds a critical value ΔB_{th} . In contrast, SC events observed against an active background ($K_p > 2$) are accompanied by impulsive absorption bursts, however small the perturbation ΔB .

Using a simple quasi-linear model we show that properties of absorption bursts, such as the dependence of their occurrence on K_p -index, the time delay between SC and absorption bursts and the existence of a threshold SC amplitude ΔB_{th} , can be explained and quantitatively predicted by the whistler cyclotron instability theory. We have investigated changes in the whistler growth rate during typical SC taking into account changes in all parameters in the relevant equation, including changes in the fraction of resonant electrons. Changes in the latter parameter are mainly due to acceleration of trapped electrons in the induction electric field. Note that an increased flux of trapped electrons with $E > 30$ keV, consistent with the betatron acceleration effect, was observed by a geosynchronous satellite during the SC event on 22 March 1979 (Wilken et al., 1986). Changes in plasma density due to the frozen-in flux condition are also taken into account.

We show that the existence of a threshold value ΔB_{th} deduced from experimental data, can be related to the existence of a threshold for exciting and maintaining the whistler cyclotron instability which is predicted by the quasi-linear theory. We find that in the quiet magnetosphere the minimum jump ΔB of magnetic field which increases the wave growth rate to the generation threshold at $L=5.3$ is close to the experimental magnitude ΔB_{th} of about 30 nT. It is clear that the minimum magnitude ΔB_{th} depends on pre-history, i.e. on the state of the magnetosphere, at a given L -shell before the SC event, in particular on the characteristics of the magnetospheric plasma (cold and hot plasma density and pitch-angle distribution function of the resonant electrons). This means that the threshold magnitude ΔB_{th} should depend on the L -shell and MLT sector. In the afternoon sector, at 14:00–18:00 MLT, where initial trapped fluxes are the lowest, the minimum jump ΔB_{th} , deduced from our calculations is about 40 nT, whereas in the morning sector it is about 25–30 nT. Note that Ortner et al. (1962) and Hartz (1963) reported local time and latitude dependences of SCA bursts, with the highest probability that they should be observed in the morning-noon sector at geomagnetic latitudes 64° – 66° .

We have also investigated changes in anisotropy, wave growth rate and diffusion coefficient during the early phase of the SC, during the SC rise time, for different assumed diffusion regimes. We have found that when the diffusion process is turned on, the wave growth saturates very quickly. The maximum growth duration is 30–15 s in the regime of weak diffusion and 3–1 s for moderate – strong diffusion, whereas the typical SC rise time is 120–180 s. Saturation corresponds to the onset of nonlinear processes within the wave-particle system. In conditions of weak diffusion the system relaxes to a new equilibrium state with a higher level of wave energy than in conditions of strong diffusion. As a result, the same perturbation ΔB has the greatest effect on the diffusion coefficient when conditions of weak diffusion prevail.

Analytical expressions describing the dependence of the diffusion coefficient and resultant absorption on the value of the magnetic field perturbation ΔB , induced by the SC and on the strength of the diffusion process (β), have been deduced. Results are presented in Table 4. This shows that the model can describe both the magnitude of observed absorption bursts ($A_{exp}(T)$) and the dependence of the absorption increase ($A_{exp}(T)/A_{exp}(t_0)$) on the SC amplitude ΔB and parameter β . Here it should be noted that the observed values of absorption correspond to a regime of weak-moderate diffusion. Moreover, the values of β , which have to be assumed to satisfy the experimental data, are found to depend on the diffusion regime existing before the SC event. If the SC occurs against a background of weak diffusion (initial precipitation is small, $A_0=0.1$ – 0.3 dB), only a weak diffusion regime is realized during SC events ($\beta=0.1$ – 0.3). When the background absorption is higher, moderate diffusion ($\beta=0.4$ – 0.6) is needed to explain the observed SCA amplitudes. Only in rare cases, when we observe strong absorption before the SC and large values of ΔB , does the diffusion during the SC become close to strong ($\beta=0.7$ – 1.0).

Further, it can be noted that the largest relative changes in measured absorption, ($A_{exp}(T)/A_{exp}(t_0)$), take place when the pitch angle diffusion is weak. For example, for ΔB about 26 nT values of relative absorption increases of 3.3, 2.5, 2.0 and 1.6 correspond to $\beta=0.3, 0.4, 0.5$ and 0.6 , respectively. As the theory predicts (Fig. 5 and Eq. (11)), in the regime of weak diffusion, the value of wave growth rate $\gamma(t)$ in a new equilibrium state is higher, and changes in diffusion coefficient are larger than in the regime of strong diffusion.

6 Summary

Bursts of cosmic noise absorption induced by a sharp jump in the magnetic field (ΔB) in the equatorial plane of the magnetosphere have been studied on the basis of a large experimental data set (about 300 events). We have shown that, for events preceded by quiet conditions, a threshold value ΔB_{th} exists below which the magnetic field perturbation does not cause a detectable absorption change. For events preceded by more active conditions the effect in absorption is observed regardless of the level of magnetic perturbation. The results are explained quantitatively in the framework of whistler cyclotron instability theory. We have shown that the minimum magnitude ΔB_{th} needed for exciting and maintaining the whistler cyclotron instability depends on pre-history, i.e. on the state of the magnetosphere at a given L -shell before the SC event, in particular on the characteristics of the magnetospheric plasma. Also, it should depend on the L -shell and MLT sector.

For events preceded by more active conditions, analytical expression describing the dependence of the diffusion coefficient and resultant absorption on the value of the magnetic field perturbation ΔB and on the strength of the diffusion process have been deduced. For 60 real events (Table 4), we have shown that the model can describe both the magnitude

Table 4. Comparison of observed and calculated cosmic-noise absorption changes for a representative subset of the events analysed. Observed quantities are dates, times (UT), magnitudes of the SC magnetic field jump (ΔB), the absorption preceding the SC ($A_{exp}(t_0)$), the absorption increase associated with the SC (ΔA) and the total absorption following the SC ($A_{exp}(T)$). β is the diffusion strength parameter which is found to be necessary to fit the observed $A_{exp}(T)$ (from the range represented in Table 3). $A_{cal}(T)$ are the calculated absorption and $A_{exp}(T)/A_{exp}(t_0)$ the relative absorption increase.

Date	UT	ΔB nT ($L=5.3$)	$A_{exp}(t_0)$ dB	ΔA dB	$A_{exp}(T)$ dB	β	$A_{cal}(T)$ dB	$A_{exp}(T)/$ $A_{exp}(t_0)$
16 April 1982	17:02	13	0.1	0.5	0.6	0.1	0.56	6.0
10 October 1988	02:31	14	0.1	0.4	0.5	0.1	0.64	5.0
1 April 1982	13:04	16	0.1	0.9	1.0	0.1	0.84	10.0
9 June 1982	00:39	30	0.1	0.5	0.6	0.2	0.73	6.0
6 October 1988	00:38	9	0.2	0.5	0.7	0.1	0.66	3.5
15 February 1980	12:34	10	0.2	0.7	0.9	0.1	0.8	4.5
9 October 1988	10:09	10	0.2	0.6	0.8	0.1	0.76	4.0
2 June 1978	09:13	11	0.2	0.7	0.9	0.1	0.86	4.5
21 February 1979	03:00	14	0.2	0.4	0.6	0.2	0.5	3.0
4 May 1989	23:52	15	0.2	0.3	0.5	0.2	0.54	2.5
4 June 1978	12:11	17	0.2	0.4	0.6	0.2	0.6	3.0
12 December 1981	01:43	19	0.2	0.4	0.6	0.2	0.7	3.0
18 September 1989	10:24	25	0.2	0.4	0.6	0.3	0.61	3.0
24 July 1970	11:26	30	0.2	0.7	0.9	0.3	0.76	4.5
5 November 1973	09:52	30	0.2	0.7	0.9	0.3	0.76	4.5
6 January 1975	19:57	35	0.2	0.7	0.9	0.3	0.94	4.5
3 February 1979	18:23	12	0.3	0.5	0–8	0.2	0.7	2.7
26 July 1979	18:33	12	0.3	0.6	0.9	0.2	0.7	3.0
6 February 1981	08:48	14	0.3	0.4	0.7	0.2	0.76	2.3
24 April 1982	20:16	17	0.3	0.5	0.8	0.2	0.93	2.7
24 April 1979	23:57	24	0.3	1.4	1.7	0.2	1.6	5.7
14 September 1985	05:58	19	0.3	0.3	0.6	0.3	0.69	2.0
1 May 1967	19:06	30	0.3	0.7	1.0	0.3	1.1	3.3
27 June 1970	06:05	32	0.3	1.0	1.3	0.3	1.24	4.3
13 April 1973	04:37	40	0.3	0.9	1.2	0.4	1.13	4.0
23 March 1969	18:27	44	0.3	0.9	1.2	0.4	1.3	4.0
10 June 1983	04:50	14	0.4	0.5	0.9	0.2	1.0	2.3
17 May 1983	00:20	15	0.4	0.9	1.3	0.2	1.1	3.3
24 May 1983	12:39	17	0.4	0.6	1.0	0.2	1.2	2.5
19 September 1967	19:59	18	0.4	0.5	0.9	0.3	0.89	2.5
13 October 1983	04:39	22	0.4	0.7	1.1	0.3	1.06	2.8
29 June 1981	06:09	26	0.4	1.0	1.4	0.3	1.3	3.5
22 October 1981	05:24	29	0.4	1.0	1.4	0.3	1.5	3.5
23 March 1966	11:33	30	0.4	0.6	1.1	0.4	1.08	2.8
12 April 1969	20:46	34	0.4	0.7	1.1	0.4	1.2	2.8
8 November 1969	18:37	40	0.4	0.8	1.2	0.4	1.5	3.0
8 November 1969	18:37	40	0.4	0.8	1.2	0.5	1.2	3.0
17 May 1969	20:59	10	0.5	0.4	0.9	0.3	0.8	1.8
23 August 1981	12:56	17	0.5	0.5	1.0	0.3	1.1	2.0
24 May 1984	08:45	25	0.5	1.1	1.6	0.3	1.5	3.2
2 February 1972	08:18	22	0.5	0.5	1.0	0.4	1.0	2.0
1 June 1970	03:05	24	0.5	0.5	1.0	0.4	1.1	2.0
13 April 1983	11:00	50	0.5	2.6	3.1	0.4	2.8	6.2

Table 4. Continued.

Date	UT	ΔB nT ($L=5.3$)	$A_{exp}(t_0)$ dB	ΔA dB	$A_{exp}(T)$ dB	β	$A_{cal}(T)$ dB	$A_{exp}(T)/$ $A_{exp}(t_0)$
3 January 1978	20:42	11	0.6	0.4	1.0	0.4	0.9	1.7
16 June 1969	06:22	15	0.6	0.4	1.0	0.4	1.0	1.7
25 July 1981	05:15	26	0.6	1.4	2.0	0.3	1.9	3.3
11 November 1979	02:25	26	0.6	0.9	1.5	0.4	1.4	2.5
12 June 1982	14:42	27	0.6	0.5	1.1	0.5	1.2	1.8
30 May 1972	14:21	32	0.6	0.5	1.0	0.5	1.17	1.7
6 June 1979	19:27	36	0.6	1.0	1.6	0.5	1.56	2.7
5 April 1979	01:55	22	0.7	0.6	1.3	0.5	1.25	1.86
17 June 1972	13:10	56	0.7	2.3	3.0	0.5	3.1	4.3
2 October 1981	2021	22	0.8	0.8	1.6	0.5	1.43	2.0
29 December 1981	0455	25	0.8	0.8	1.6	0.5	1.55	2.0
6 July 1979	1930	24	0.8	0.5	1.3	0.6	1.36	1.6
2 May 1969	1811	43	0.8	1.3	2.1	0.6	2.1	2.6
28 April 1971	13:06	40	1.0	1.1	2.3	0.7	2.1	2.3
04 October 1983	05:42	13	2.2	0.6	2.8	0.7	2.8	1.3
10 May 1981	22:08	20	2.2	1.3	3.6	0.7	3.4	1.6
24 July 1970	23:47	65	3.5	5.1	8.6	1.0	8.3	2.4

of observed absorption bursts and the dependence of the absorption increase on ΔB and a parameter β . For a given ΔB , the values of β , which satisfy the experimental data, depend on the diffusion regime existing before the SC event. As can be seen in Table 4, weak to moderate diffusion regimes are realized during most of the SC events ($\beta=0.1-0.6$).

Thus, we find that the quasi-linear whistler-cyclotron instability model is well able to explain both qualitative and quantitative features of cosmic-noise absorption bursts associated with sudden commencements of geomagnetic storms.

Appendix A

Calculation of SC-amplitude in the magnetosphere

We determine the value of the perturbation ΔB in magnetic field strength, in the equatorial magnetosphere at the L -shell corresponding to the riometer station Loparskaya ($L=5.3$) using both the amplitude, ΔH , measured at the Earth's surface and information on the variation of solar wind parameters at the front of the bow shock obtained from the satellites IMP-8 and WIND.

It is known that a sharp increase in dynamic pressure, P_d , of the solar wind on the magnetosphere acts to compress the magnetosphere. This effect is displayed in variations of the magnetic field inside the magnetosphere, both at satellite altitudes and at the Earth's surface. Such impulses seen at the Earth's surface have long been identified as "sudden impulses" or "sudden commencements" when followed by a geomagnetic storm. The physical reason for the effect is an increase in the Chapman-Ferraro currents. At the Earth's sur-

face, at stations located near equator, the effect of the shock is seen as a sharp increase, ΔH , of the horizontal component of geomagnetic field. To evaluate ΔB we apply the following formulae obtained in accordance with Mead (1964) and Siscoe (1966):

$$\Delta B = B_{CFI} - B_{CFP} = B_{CFP} \{ (P_{S2}/P_{S1})^{1/2} - 1 \} \quad (\text{A1a})$$

$$\Delta B = \frac{2}{3} \frac{B_{CFP}}{B_{CFPE}} \frac{\Delta H}{\cos \varphi}, \quad (\text{A1b})$$

where P_{S1} , P_{S2} are the dynamic pressure of the solar wind before the shock wave passes and at the front of the shock wave or discontinuity, respectively. ($P_S = k\rho V_{SW}^2$, $\rho \equiv m_p n_p$, where ρ is the density of the solar wind; V_{SW} is the velocity of the solar wind; $k \cong 1$); B_{CFPE} and B_{CFP} are the horizontal components of the magnetic field due to the Chapman-Ferraro currents at the plane of the geomagnetic equator at the Earth's surface and at distance r (in Earth radii) in the magnetosphere for conditions corresponding to the quiet solar wind, B_{CFI} is the value of the field due to the Chapman-Ferraro currents at the same place as B_{CFP} but during the disturbance; ΔH is the amplitude of the SC at the Earth's surface at latitude φ .

The values of the SC-amplitude at $L=5.3$ (Table 1) obtained with Eq. (A1a), on the basis of measurements of the solar wind parameters by IMP-8, and Eq. (1b) using ΔH values measured at the station Alibag ($\varphi=18.6^\circ$ N, $\lambda=72.9^\circ$ E; $\Phi'=12.4^\circ$ N, $\Lambda=142.9^\circ$ E) are in good agreement. Magnetic fields of the Chapman-Ferraro currents, B_{CFPE} and B_{CFP} , are calculated in the given geomagnetic local time sector in accordance with Mead (1964) and Siscoe (1966).

Acknowledgements. Topical Editor T. Pulkkinen thanks S. Samsonov and another referee for their help in evaluating this paper.

References

- Binsak, J. H.: Plasmapause observations with MLT experiment on Imp-2., *J. Geophys. Res.*, 72, No. 21, 5231–5237, 1967.
- Brown, R. R., Hartz, T. R., Landmark, B., Leinbach, T., and Ortner, J.: Large-scale electron bombardment at the atmosphere at the sudden commencement of geomagnetic storm., *J. Geophys. Res.*, 66, 1035, 1961.
- Carpenter, D. L.: Relations between the dawn minimum in the equatorial radius of the plasmapause and D_{st} , K_p and local K at Byrd station., *J. Geophys. Res.*, 72, No. 11, 2969–2971, 1967;
- Carpenter, D. L., Chappel, C. R.: Satellite studies of magnetospheric substorm on August 15, 1968., *J. Geophys. Res.*, 78, No. 16, 3602–3607, 1973.
- Chappel, C. R., Harris, K. K., Sharp, G. W.: A study of the influence of magnetic activity of the local of the plasmapause as measured by Ogo-5, *J. Geophys. Res.*, 75, No.1, 50–56, 1970a.
- Chappel C. R., Harris, K. K., Sharp, G. W.: The morphology of the bulge region of the plasmasphere, *J. Geophys. Res.*, 75, No. 19, 3848–3861, 1970b.
- Chappel, C. R., Harris, K. K., and Sharp, G. W.: The dayside of the plasmasphere, *J. Geophys. Res.* 76, 7632–7647, 1971.
- Collis, P. N., Hargreaves, J. K., Korth, A.: Loss cone fluxes and pitch angle diffusion at the equatorial plane during auroral radio absorption events., *Planet. Space Sci.*, 45, No. 4, 231–245, 1983.
- Coroniti, V. F. and Kennel, C. F.: Electron Precipitation Pulsations, *J. Geophys. Res.*, 75, 7, 1279–1289, 1970.
- Cornilleau-Wehrlin, N., Solomon, J., Korth, A., and Kremser, G.: Experimental study of the relationship between energetic electrons and ELF waves observed on board GEOS: A support to quasi-linear theory, *J. Geophys. Res.*, 90, No. A5, 4141–4154, 1985.
- Davidson, G. T. and Chiu, Y. T.: A closed nonlinear model of wave-particle interactions in the outer trapping and morningside auroral regions, *J. Geophys. Res.*, 91, A12, 13 705–13 710, 1986.
- Davidson, G. T., Filbert, P., Nightingale, C. R. W., Imhof, W. L., Reagon, J. B., and Whipple, E. C.: Observations of intense trapped electron fluxes at synchronous altitudes. *J. Geophys. Res.*, 93, A1, 77–95, 1988.
- Demekhov, A. G., and Trakhtengerts, V. Y.: A mechanism of formation of pulsating aurorae, *J. Geophys. Res.*, 99, A4, 5831–5841, 1994.
- Demekhov A. G., Lyubchich, A. A., Trakhtengerts, V. Y., Titova, E. E., Manninen, J., and Turunen, T.: Modeling of nonstationary electron precipitation by the whistler cyclotron instability, *Ann. Geophys.*, 16, 1455–1460, 1998.
- Erlanson R. E., Sibeck, D. G., Lopez, R. E., Zanetti, L. J., and Potemra, T. A.: Observations of solar wind pressure initiated fast mode waves at the geostationary orbit and in polar cap, *J. Atmos. Terr. Phys.*, 53, 231–239, 1991.
- Etcheto J., Gendrin, R., Solomon, J., and Roux, A.: A self-consistent theory of magnetospheric ELF hiss, *J. Geophys. Res.*, 78, 34, 8150–8165, 1973.
- Gail, W. B., Inan, U. S., Helliwell, R. A., Carpenter, D. L., Krisnaswamy, S., Rosenberg, T. J., and Lanzerotti, L. J.: Characteristics of wave-particles interactions during sudden commencements, 1. Ground-based observations, *J. Geophys. Res.*, 95, A1, 119–137, 1990.
- Gail, W. B. and Inan, U. S.: Characteristics of wave-particles interactions during sudden commencements, 2. Spacecraft observations, *J. Geophys. Res.*, 95, A1, 139–147, 1990.
- Harris, K. K., Sharp, G. W., and Chappel, C. R.: Observation of the plasmapause from OGO-5, *J. Geophys. Res.*, 75, No. 1, 219–224, 1970.
- Hartz, T. R.: Multistation riometer observations in Radio Astronomical and Satellite Studies of the Atmosphere, edited by Aarons, J., North Holland, Amsterdam, 220–237, 1963.
- Haugstad, B. C.: Modification of the theory of electron precipitation pulsations., *J. Atmos. Terr. Phys.*, 37, 257–272, 1975.
- Hayashi, K., Kokubun, S., and Ogoti, T.: Polar chorus emission and worldwide geomagnetic variation, *Rep. Ionos. Space Res. Jpn.*, 22, 149, 1968.
- Kennel, C. F. and Petschek, H. E.: Limit of stably trapped particle fluxes, *J. Geophys. Res.*, 71, 1, 1–28, 1966.
- Kirkwood, S. and Osepian, A.: Pitch-angle diffusion coefficients and precipitating electron fluxes inferred from EISCAT radar measurements at auroral latitudes, *J. Geophys. Res.*, 106, A4, 5565–5578, 2001.
- Kivelson, M. G., Farley, T. A., and Aubry, M. P.: Satellite studies of magnetospheric substorm on August 15, 1968, 5. Energetic electrons, spatial boundaries and wave-particle interactions at OGO 5., *J. Geophys. Res.*, 78, 16, 3079–3092, 1973.
- Kleimenova, N. G. and Osepian, A. P.: VLF emissions at the time of sudden commencements (in Russian), *Geomagn. and Aeronomy*, XXII, No. 4, 681–683, 1982.
- Kokubun S.: Characteristics of storm sudden commencement at geostationary orbit., *J. Geophys. Res.*, 88, 10 025, 1983.
- Laakso, H. and Schmidt, R.: Pc4-5 pulsations in the electric field at geostationary orbit (GEOS 2) triggered by suddern storm commencements, *J. Geophys. Res.*, 94, A6, 6626–6632, 1989.
- Lyons, L. R., Williams, D. J.: The quiet time structure of energetic (35–560 keV) radiation belt electrons., *J. Geophys. Res.*, 80, 7, 943–949, 1975.
- Mal'tsev, Yu. P.: Electric field induced in the magnetosphere by sudden impulse, *Geomagn. and Aeronom.*, v. 1, 23–26, 1998.
- Manninen J., Turunen, T., Lubchich, A., Titova, E., and Yahnina, T.: Relations of VLF emissions to impulsive electron precipitation measured by EISCAT radar in the morning sector of auroral oval, *J. Atmos. and Terr. Phys.*, 58, No. 1–4, 97–106, 1996.
- Mead, G. D.: Deformation of the geomagnetic field by the solar wind., *J. Geophys. Res.*, 69, 7, 1181–1195, 1964.
- Morgan, M. G. and Maynard, N. C.: Evidence of dayside plasmaspheric structure through comparisons of ground-based whistler data and Explorer-45 plasmapause data, *J. Geophys. Res.*, 81, 22, 3922–3928, 1976.
- Morozumi, H. M.: Enhancement of VLF chorus and ULF at the time of SC., *Rep. Ionos. Space Res. Jpn.*, 19, 371, 1965.
- Nopper R. W., Jr., Hugher W. J., MacLennan C. G. and McPherron R. L.: Impulsive-excited pulsations during the July 29, 1977, event. *J. Geophys. Res.*, 87, No. A8, 5911–5916, 1982.
- Ortner, J. B., Hultqvist, B., Brown, R. R., Hartz, T. R., Holt, O., Landmark, B., Hook, J. L., and Leinbach, H.: Cosmic noise absorption accompanying geomagnetic storm sudden commencement, *J. Geophys. Res.*, 67, 4169, 1962.
- Osepian A.: Betatron acceleration at the time of SC events. Investigations of geomagnetism and aeronomy in the auroral zone (in Russian), *Science*, 186–193, 1973.
- Park, C. G., Carpenter, D. L., and Wiggins, D. B.: Electron density in the plasmasphere : whistler data on solar cycle, auroral and diurnal variations, *J. Geophys. Res.* 83, 3137–3144, 1978.

- Perona, G. E.: Theory on the precipitation of magnetospheric electrons at the time of sudden commencements, *J. Geophys. Res.*, 77, 101–111, 1972.
- Potemra, T. A., Lühr, H., Zanetti, L. J., Takahashi, K., Erlandson, R. E., Marklund, G. T., Block, L. P., Blomberg, L. G., and Lepping, P. P.: Multi-satellite and ground-based observations of transient ULF wave, *J. Geophys. Res.*, 94, A3, 2543–2554, 1989.
- Reeves, G. D.: Energetic particle observations at geosynchronous orbit, *Proceeding of the International Workshop on Magnetic Storms*, edited by Kamide, Y., *Sol. Terr. Environ.*, Nagoya, Japan, 1994.
- Rycroft, M. J. and Thomas, J. O.: The magnetospheric plasmopause and the electron density through at the Alouette II orbit., *Planet. Space Sci.*, 18, 1, 65–80, 1970.
- Singh, N., Horwitz, J. L.: Plasmasphere refilling: Recent observations and modeling., *J. Geophys. Res.*, 97, No. A2, 1049–1079, 1992.
- Siscoe, G. L.: A unified treatment of magnetospheric dynamics with applications to magnetic storms., *Planet. Space Sci.*, 1966, v. 14, 10, 947–963, 1966.
- Schulz M. and Davidson, G.: Limiting energy spectrum of a saturated radiation belt., *J. Geophys. Res.*, 93, 1, 59–76, 1988.
- Thorolfsson A., Cerisier, J. C., and Pinnock, M.: Flow transients in the postnoon ionosphere: The role of solar wind dynamic pressure, *J. Geophys. Res.*, 106, A2, 1887–1901, 2001.
- Trakhtengerts, V. Y., Tagirov, V. R., and Chernouss, S. A.: A circulating cyclotron maser and pulsed VLF emissions, *Geomagn. and Aeronom.*, 26, 77–82, 1986.
- West Jr., H. I., Buck, R. M., and Walton, J. R.: Electron pitch angle distribution throughout the magnetosphere as observed on OGO 5., *J. Geophys. Res.*, 78, 7, 1064–1081, 1973.
- Wilken, B., Baker, D. N., Higbie, P. R., Fritz, T. A., Olson, W. P., and Pfizter, K. A.: The SSC on July 29, 1977 and its propagation within the magnetosphere, *J. Geophys. Res.*, 87, No. A8, 5901–5910, 1982.
- Wilken, B., Baker, D. N., Higbie, P. R., Fritz, T. A., Olson, W. P., and Pfizter K. A.: Magnetospheric configuration and energetic particle effects associated with SSC: A case study of the CDAW 6 event on March 22, 1979, *J. Geophys. Res.*, 91, No. A2, 1459–1473, 1986.
- Yahnin, A., Titova, E., Lubchich, A., Böisinger, T., Manninen, J., Turunen, T., Hansen, T., Troshichev, O., and Kotikov, A.: Day-side high latitude magnetic impulsive events: their characteristics and relationship to sudden impulses, *J. Atmos. Terr. Phys.*, 57, 13, 1569–1582, 1995.